International Journal of Science and Research (IJSR)
ISSN (Online): 2319-7064
Index Copernicus Value (2016): 79.57 | Impact Factor (2015): 6.391

Time Evolution of thePlasma Produced by the Single Dielectric Barrier Discharge Plasma Actuator

Thamir H. Khalaf[1], Dawser H. Ghayb[2]

[1]Department ofPhysics, College of Science, Baghdad University, Baghdad, Iraq.

[2]Department ofPhysics, College of Science for Women, Baghdad University, Baghdad, Iraq

Abstract: ***The main aim of the present paper is to study the plasma produced by DBD plasma actuator through follow the time evolution of the electric potential, electron density, and ions density. Airlike mixture consists of Nitrogen and Oxygen gases were used as a discharge gas. An AC voltage applied to the actuator to drive the plasma. Simulations have been performed to understand the plasma produced. A fluid model was usedas a simulation model. A two dimensional simulation of the actuator geometry used and finite element method solved in COMSOL multiphysics software were done. The duration of the simulated discharge is in the range of nanoseconds. The resultant parameters from the actuator are seen as a function of applied voltage amplitude. Results show that there is an increasing in the electric potential as the time evolved. In addition to that, and as the time increased, electron density and ions density also increased in value and spread along the dielectric surface.***

Keywords: electric potential, ion density, electron density, plasma actuator

1. Introduction

Plasma actuators refer to a broad class of devices that use high voltage electrical discharges to provide an induced momentum on fluid. There are various classes of actuators derived from the class of electrical discharge such as: direct discharge, microwave discharge, DBD, corona discharge, spark, etc. [1 - 2]. The Dielectric Barrier Discharge (DBD) plasma actuator is the commonly used plasma actuator. It typically consists of a set of asymmetrically placed electrodes and a dielectric. One of the main advantages of the DBD plasma actuator technique is the absence of moving parts. This enhances reliability and maintenance greatly, no middle agent between the conversions of electric energy into kinetic energy is required, which removes losses in this intermediate step, following from the previous point, the response time is very short. This enables high frequency real-time flow control. The DBD actuators have a wide bandwidth and can operate over a wide range of actuation frequencies [3].DBD plasma actuators are used in many applications. Some of the applications investigated include active stall detection and control system [4], bluff body noise control [5], plasma-enhanced combustion [6], jet mixing enhancement [7] and DBD microthrusters [8].

Many experimental and numerical works have been done for the purpose of better understanding the mechanisms by which these kinds of actuators influence the flow and also for the optimization of their design and improvement of their performance [9-11]. In the present work, a study of the plasma produced in a plasma actuator through the time evolution of the electric potential, ions density, and electron density.

2. Plasma Model

The modeled gas was air consisting of neutrals, electrons, positive, and negative ions. The air was considered as a mixture of oxygen and nitrogen gases with percent 22:78% respectively.The model used in the present work is the fluid model. Solving the drift-diffusion equations will results in compute the electron density and mean electron energy. The drift diffusion equations set are [12 - 13]:

$$\frac{dn_e}{dt} + \nabla.\Gamma_e = R_e - (u.\nabla)n_e \quad \text{.....(1)}$$

$$\Gamma_e = -(\mu_e.E)n_e - \nabla(D_e n_e) \quad \text{.....(2)}$$

$$\frac{\partial}{\partial t}(n_e) + \nabla.\Gamma_\varepsilon + E.\Gamma_e = R_\varepsilon - (u.\nabla)n_\varepsilon \quad \text{.....(3)}$$

$$\Gamma_\varepsilon = -(\mu_\varepsilon.E)n_\varepsilon - \nabla(D_\varepsilon n_\varepsilon) \quad \text{.....(4)}$$

Where: n_e is the electron density ($1/m^3$), n_ε is the ion density ($1/m^3$), Γ_e is the secondary emission energy flux ($V/m^2.s$), μ_e is the electron mobility, R_e is the electron source and R_ε is the energy loss due to inelastic collisions.

The ion number density, or specie k number density, is given by:

$$n_k = \left(\frac{P}{K_\beta T}\right) x_k \quad \text{..... (5)}$$

Where: P(SI unit: Pa) is the absolute pressure of the fluid.
The electron diffusivity, energy mobility, and energy diffusivity are computed from the electron mobility using the relations:

$$D_e = \mu_e.T_e \quad \text{.....(6)}$$

Where: T_e = Electron temperature. To compute the ion mobility μ_ε the following equation is used:

$$\mu_\varepsilon = 5 / 3\ \mu_e \quad \text{.....(7)}$$

While the ion diffusivity D_ε related to the ion mobility by the relation:

$$D_\varepsilon = \mu_\varepsilon.T_\varepsilon \quad \text{.....(8)}$$

The source coefficients in the above equations are determined by the plasma chemistry using rate coefficients. If we have

Mreactions that contribute to the growth or decay of electron density and A is considered as theinelastic electron-neutral collisions, since theinelastic electron-neutral collisions are much larger thanreactions that contribute to the growth or decay of electron density (in general)then electron source term is given by:

$$R_e = \sum_{j=1}^{m} x_j k_j N_n n_e \quad \text{.....(9)}$$

Where:$x_j$is the mole fraction of the target species for reaction *j*, $k_j$is the rate coefficient for reaction j(m^3/s), and $N_n$is the total neutral number density ($1/m^3$). The electron energy loss is obtained by the summationof the collisional energy loss over all reactions:

$$R_\varepsilon = \sum_{j=1}^{A} x_j k_j N_n n_e \Delta\varepsilon_j \quad \text{.....(10)}$$

Where:$\Delta\varepsilon_j$is the energy loss from reaction j(V). The rate coefficients can be computed from cross-section data using the equation:

$$K_k = \gamma \int_0^\infty \varepsilon \sigma_k(\varepsilon) f(\varepsilon)\, d\varepsilon \quad \text{.....(11)}$$

Where: $\gamma = (2q/m_e)^{1/2}$ ($C^{1/2}/kg^{1/2}$), $m_e$is the electron mass (kg), ε is the energy (V), $\sigma_k$is the collision cross section (m^2), and fis the electron energy distribution function. For the non-electron species, suppose a reacting flow consists of $k = 1, \ldots, Q$ species and $j = 1, \ldots, N$ reactions. The equation for the first *Q*-1 species is given by:

$$\rho \frac{\partial}{\partial t}(w_k) + \rho (\mathbf{u} \cdot \nabla) w_k = \nabla \cdot \mathbf{j}_k + R_k \quad \text{.....(12)}$$

where: $\mathbf{j}_k$is the diffusive flux vector, $R_k$is the rate expression for species *k* (SI unit: kg/(m^3·s)), **u** is the mass averaged fluid velocity vector (SI unit: m/s), ρ denotes the density of the mixture (SI unit: kg/m^3), and $w_k$is the mass fraction of the k_{th} species (1).

The electrostatic field is computed using the equation [12]:

$$-\nabla \cdot \varepsilon_0 \varepsilon_r \nabla V = \rho \quad \text{.....(13)}$$

Where: ρ is the space charge density (C/m^3), V is the potential.

3. Boundary Conditions

Electrons are lost to the wall due to random motion within a few mean free paths of the wall and gained due to secondary emission effects, resulting in the boundary conditions:

$$-n \cdot \Gamma_e = (1/2\, v_{e,the} n_e) - \Sigma \gamma_p (\Gamma_p \cdot n) \quad \text{....(14)}$$

$$-n \cdot \Gamma_\varepsilon = (5/6\, v_{e,the} n_e) - \Sigma \varepsilon_p \gamma_p (\Gamma_p \cdot n) \quad \text{....(15)}$$

Equation (14) is for electron flux and equation (24) for the electron energy flux. The second term on the right-hand side of eq. (14) is the gain of electrons due to secondary emission effects, $\gamma_p$being the secondary emission coefficient. The second term in eq.15 is the secondary emission energy flux, $\varepsilon_p$being the mean energy of the secondary electrons.For ions, they are lost to the wall due to surface reactions and the fact that the electric field is directed towards the wall. The discharge is driven by the electric potential applied to the anode boundaries. The applied potential equation isa pulse voltage of the form[12]:

$$V = V_0 \tanh(t/\tau) \quad \text{..... (16)}$$

Where: V_0 is the amplitude to the potential (in V)

The bottom face of the dielectric is grounded. Surface charge accumulation is added to the dielectric surfaces. The surface charge density, which is $\rho_s$is computed by solving the following distributed ordinary differential equation on the surfaces[12]:

$$\frac{d\rho_s}{dt} = \mathbf{n_i} \cdot \mathbf{J_i} + \mathbf{n_e} \cdot \mathbf{J_e} \quad \text{..... (18)}$$

Where: J_i is the ion current density (A/m^3), n_i is ion density ($1/m^3$), n_e is the electron density ($1/m^3$),J_e is the electron current density (A/m^3), $n_i \cdot J_i$is the normal component of the total ion current density at the wall, and $n_e \cdot J_e$is the normal component of the total electron current density at the wall.

To sustain the simulation, initial values for electron density and electron energy were set. The initial electron density is set to be 1×10^{10}, while the mean electron energy is set to 1 eV [14].

The simulation was done using COMSOL multiphysics with finite element method as a solution method. The domain of simulation is $(0.5\times1)mm^2$. The mesh used is triangular element. Thetotal number of triangular elements 115812 element; the minimum element equality was equal to 0.7383. The element size was the smallest at the upper electrodes edges. The maximum element size was 0,001 mm (1μm) on the edge of the exposed electrode, and the minimum element size was 0.02 μm in the same region. Figure (1) shows longitudinal cross section of the plasma actuator schematic design that is proposed in the present work.

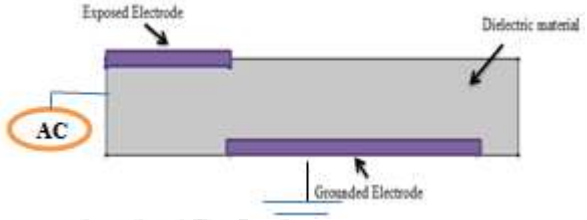

Figure 1: Schematic drawing to the cross section of SDBD plasma actuator in the present simulation.

4. Results and Discussion

The results of the present study were obtained using pulse voltage of amplitude 3 kV with rising time equal to 4 ns. The results included the electric potential, O_2 and N_2 positive ions density, and the electron density.

Electric potential:

The electric potential was calculated using Poison equation.Figure (2)shows electric potential surface distribution on the cross section of the actuator domain (V).As clear from figure, the potential increased with time until it reaches the maximum value (amplitude). Then, it spreads on the dielectric surface. This because of that the electric field is high at the exposed electrode and increased in strength as the applied voltage amplitude increased. As the voltage reached the amplitude value, the gas ionization on top of the insulated surface will result in the formation of visible plasma.

Electron density: Figure (3) shows Time evolution of the electrons density surface distribution on the cross section of the actuator domain ($1/m^3$). As the voltage increases, the

electric field at the edge of the exposed electrode increases. This causes the generation of two processes which are Townsend breakdown and photoionization, and a plasma flow is formed (streamer). The streamer propagates on the dielectric surface. The head of the streamer is above the surface of the dielectric. The streamer is being led by Townsend ionization and photoionization, both of which are caused primarily by the electrons. In fact, the electron components in a gas discharge are the carrier of energy taken from the electric field. Its energy distribution function, EEDF, and density, determine the rates at which the ionization, vibrational and electronic excitation, dissociation and all inelastic processes take place.

Ion O_2+ Density: The oxygen gas operates as a quencher of electron and molecules, resulting in the density increases of species as well as electrons. O_2 ions are the dominant between other species during discharge, due to the low ionization energy of oxygen (~ 12 V) [15].Figure (4) shows the O_2^+ ion density surface distribution on the cross section of the actuator domain ($1/m^3$). Results show thatthe ion density increased with time development. Also, it propagated along the dielectric surface. When the applied voltage amplitude rises and reaches breakdown value, the process of ionization occurs, produced a cloud of high positive ions densities. As the time increased, the voltage amplitude increased until reached the maximum value, this cloud increased in diameter and spread distance, propagates along the dielectric material while charging its surface away from the exposed electrodebecause of that the applied voltage is positive.

N_2+ Ion Number Density: N_2 positive ion number density calculated using equation (11). N_2^+ Ion Density surface distribution on the cross section of the actuator domain ($1/m^3$) for different simulation time is shown in figure (5). The number density increased as time increased. The streamer begins to spread as the voltage increased with time. It seems to be that there is a linear relationship between voltage value and the positive ion number density. Notice that N_2^+ and O_2^+ ions are response to the electric field in the same manner because both of them are positive ions, hence, their density profile are similar. N_2^+ ion density is higher than that of O_2^+. This is because of the difference in their percent in the parent gas molecules and the rate coefficient.

5. Conclusions

1) The electric potential increased as the time of simulation increased.
2) Electron density, O_2 positive ion and N_2 positive ion were increased wit time, and spread along the dielectric surface.
3) The electrons and ions composited a streamer that is started from the tip of the exposed electrode and propagate along the dielectric surface.

References

[1] J.S. Oh, O.T. Olabanji, C. Hale, R. Mariani, K. Kontis, and J.W. Bradley, “Imaging gas and plasma interactions in the surface-chemical modification of polymers using micro-plasma jets”, Journal of Physics D: Applied Physics, 44:155 - 206, 2011.
[2] E. Moreau, C. Louste, and G. Touchard, “Electric wind induced by sliding discharge in air at atmospheric pressure”, *Journal of Electrostatics*, 66:107-114, 2007.
[3] S.R. Bal, “Investigating the influence of DBD plasma actuators on skin Friction: Application to Integral Boundary Layer Formulation”, European Wind Energy Master, Delft University of Technology, Ris- Denmark Technical University, p.p.: 11 – 12, 2015.
[4] M. Samimy, J. H. Kim, J. Kastner, I. Adamovich, and Y. Utkin, “Active control of high-speed and high-Reynolds-number jets using plasma actuators,” *J. Fluids Mech.*, vol. 578, pp. 305–330, Apr. 2007.
[5] P. Gnemmi, R. Charon, J. P. Duperoux, and A. George, “Feasibility study for steering a supersonic projectile by a plasma actuator,” *AIAA J.*, vol. 46, no. 6, pp. 1308–1317, Jun. 2008.
[6] P. Q. Elias, B. Chanetz, S. Larigaldie, and D. Packan, “Study of the effect of glow discharges near am = 3 bow shock,” *AIAA J.*, vol. 45, no. 9, pp. 2237–2245, Sep. 2007.
[7] E. Moreau, L. Léger, and G. Touchard, “Effect of a DC surface non- thermal plasma on a flat plate boundary layer for airflow velocity up to 25 m/s,” *J. Electrostat.*, vol. 64, no. 3/4, pp. 215–225,Mar. 2006.
[8] J. R. Roth, D. M. Sherman, and S. P. Wilkinson, “Electro hydrodynamic flow control with a glow-discharge surface plasma,” *AIAA J.*, vol. 38, no. 7, pp. 1166–1172, Jul. 2000.
[9] H. Nishida, T. Abe, Numerical analysis of plasma evolution on dielectric barrier discharge plasma actuator, J. Appl. Phys. 110 (2011) 013302.
[10] T. Shao, H. Jiang, C. Zhang, P. Yan, M.I. Lomaev, V.F. Tarasenko, Time behavior of discharge current in case of nanosecond-pulse surface dielectric barrier discharge, EPL Europhys. Lett. 101 (2013) 45002.
[11] J.A. Valerioti, T.C. Corke, Pressure dependence of dielectric barrier discharge plasma flow actuators, AIAA J. 50 (2012) 1490-1502.
[12] COMSOL multiphysics user guide, Heavy Species Transport Theory, V4.3a. 2012. COMSOL Plasma Module User Guide, v.4.3a, 2012.
[13] aM.Mamunuru, S. Guo, D. Poon, D. Burman, T. Simon, Douglas Ernie and UweKortshagen, Separation Control using plasma actuator: Simulation of plasma actuator, 39th AIAA Fluid Dynamics Conference, 22 - 25 June 2009, San Antonio, Texas.

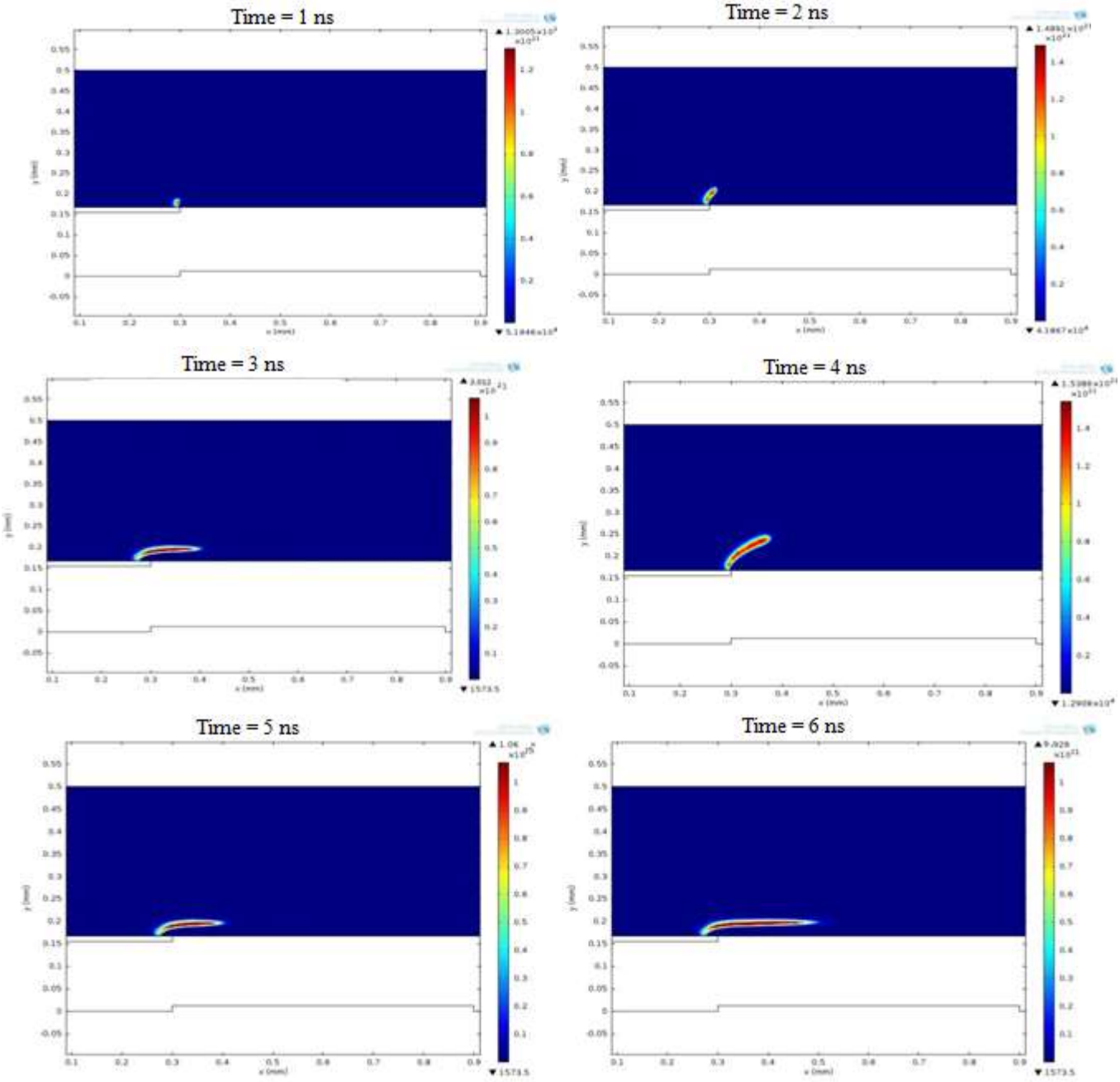

Figure 3: Time evolution of the electrons density surface distribution on the cross section of the actuator domain ($1/m^3$).

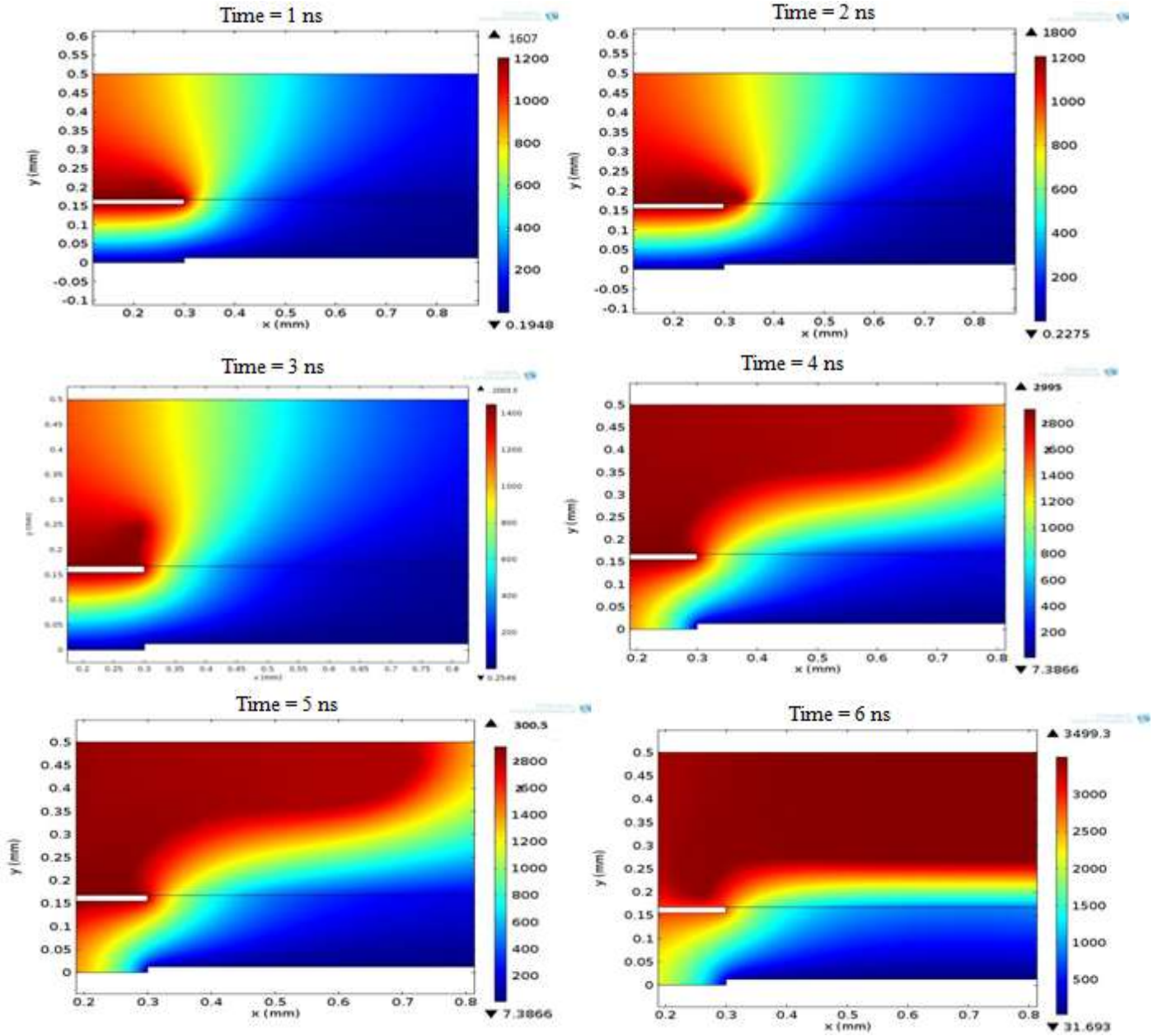

Figure 2: Time evolution of the electric potential surface distribution on the cross section of the actuator domain (V) .

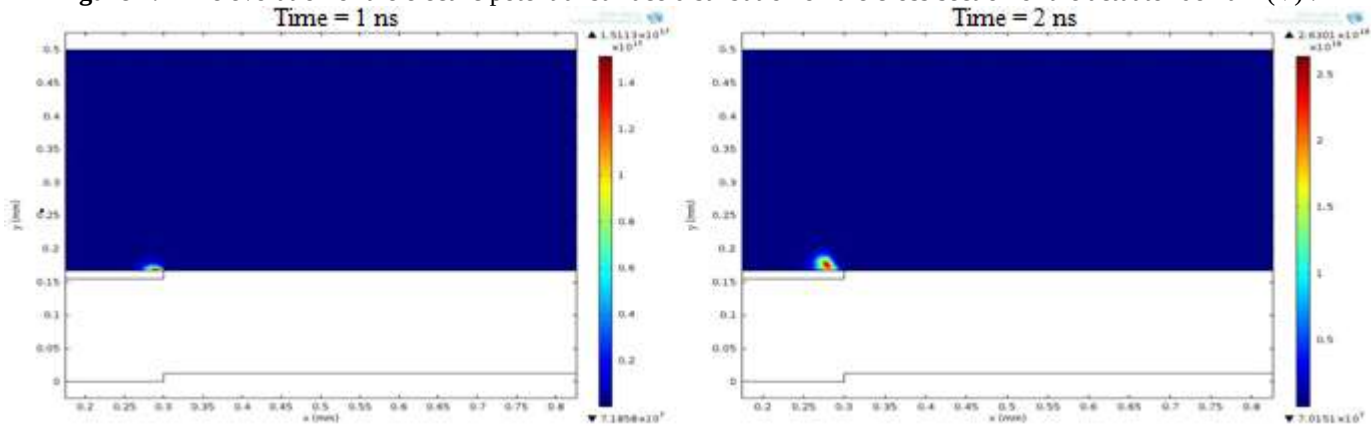

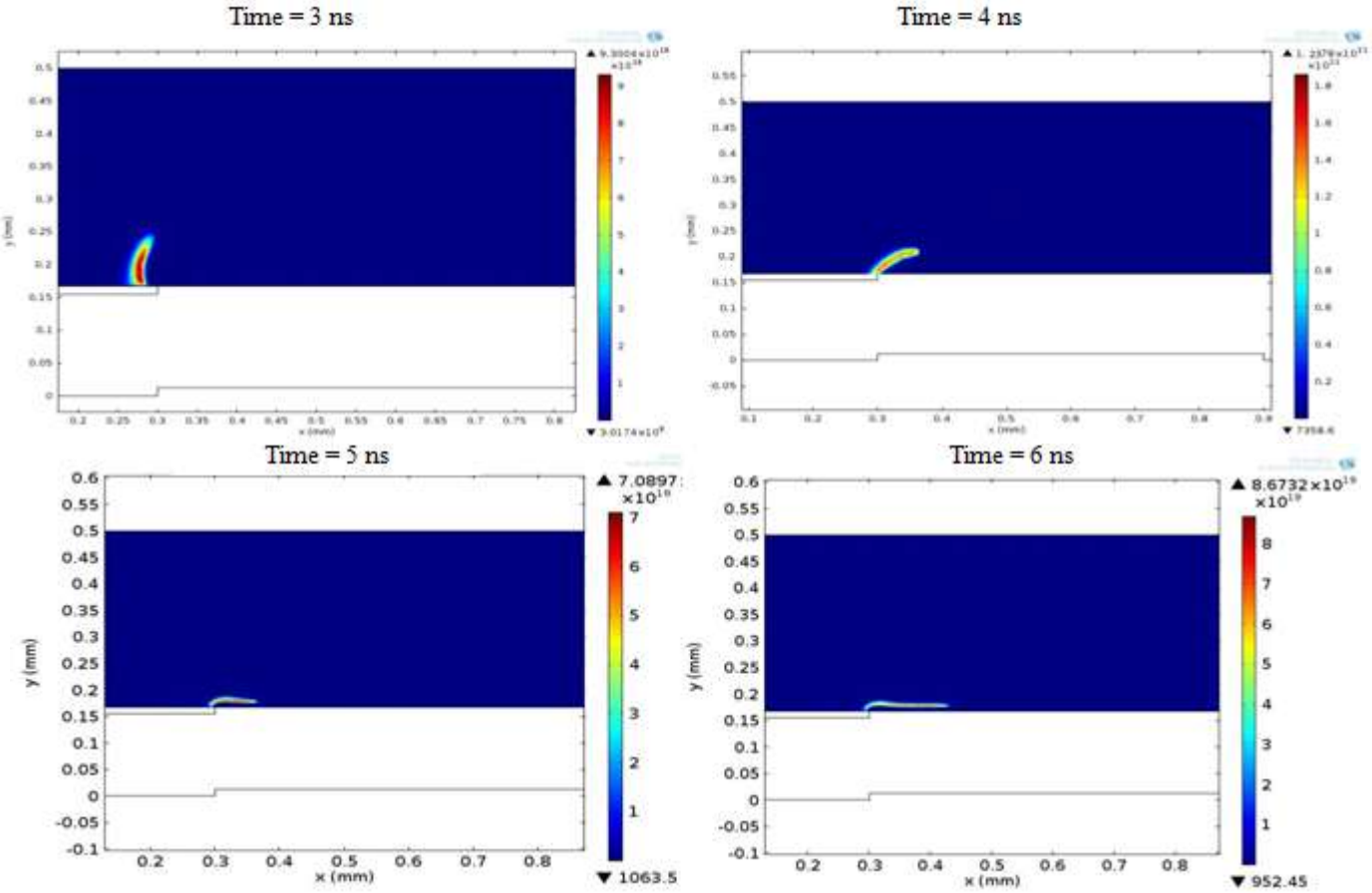

Figure 4: Time evolution of the O_2^+ ion density surface distribution on the cross section of the actuator domain ($1/m^3$)

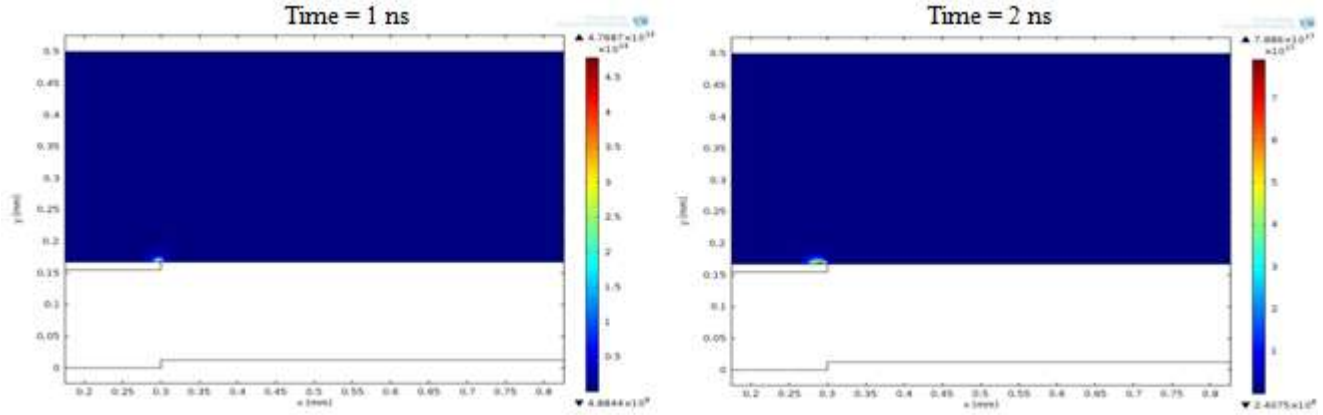

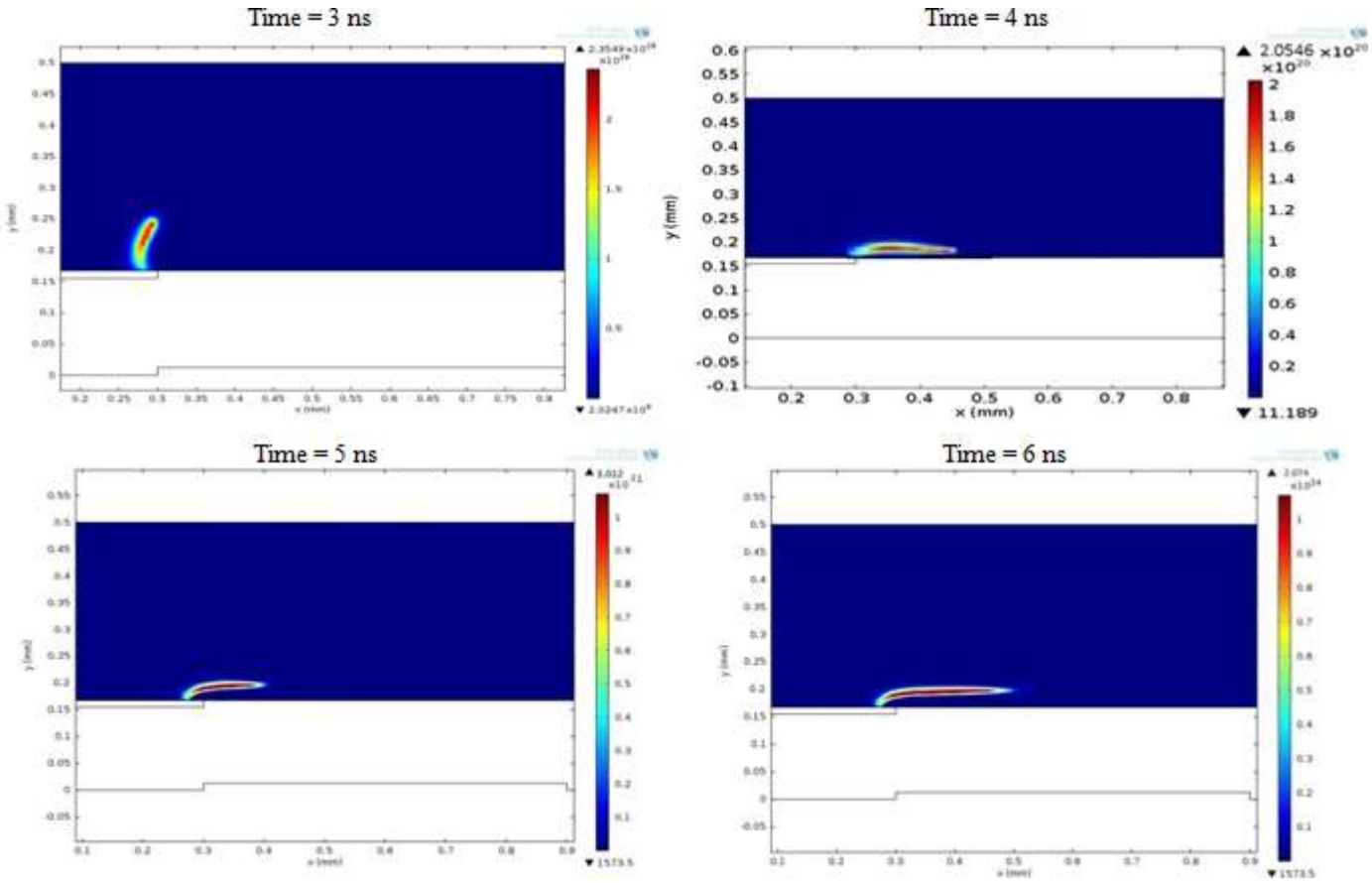

Figure 5: Time evolution of the ion N_2^+ density surface distribution on the cross section of the actuator domain ($1/m^3$).